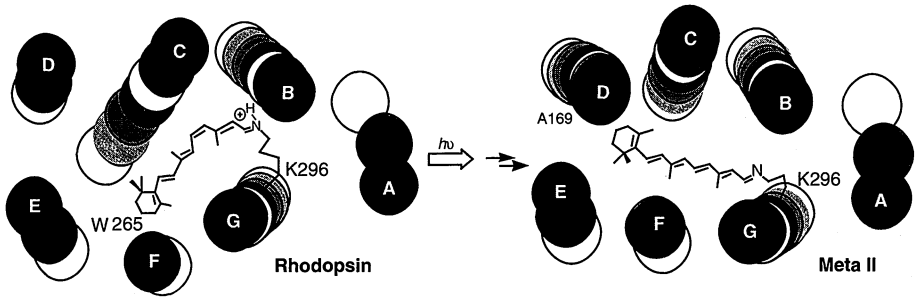

Fig. 5. A highly qualitative depiction of opsin conformational movements triggered by 11-*cis* to all-*trans* photoisomerization of the chromophore. In Rh and batho-Rh, the ionone ring is close to Trp^{265} in helix F, but in Lumi-Rh it flips over with concomitant changes in helical structures and resides close to Ala^{169} in helix D.

lumi-Rh state. Ala^{169}, an amino acid in helix D presumed not to be close to the retinal binding site, is cross-linked in the lumi-, meta-I-, and meta-II-Rh stages. This requires a movement of helices (Fig. 5) and would necessarily alter conformations of the cytoplasmic loops connecting helices C/D and E/F, which have been implicated in transducin activation (*9, 12*). It is proposed that Trp^{265} keeps 11-*cis*-retinal as an inverse agonist; thus, it is not surprising to see Trp^{265} in close proximity to the β-ionone ring both in Rh, the resting stage, and in batho-Rh, the first high-energy intermediate, while the ring moiety has flipped over in the more relaxed lumi-Rh and further intermediates.

The femtosecond photoisomerization of 11,12-ene leading to photo-Rh (Fig. 1) (*37, 38*) and then to batho-Rh does not involve movement of the ionone ring moiety; the highly strained all-*trans* polyene system gives rise to the red-shifted absorption. In the batho- to lumi-Rh step, the stored energy is dissipated by flip-over of the β-ionone ring as well as relaxation of the opsin so that helix D and Ala^{169} are situated near C-3 of the chromophore. In subsequent steps, lumi- to meta-I- to meta-II-Rh, the helical movements change conformations of the extramembrane loops connecting C/D and E/F helices, but the environment surrounding the β-ionone does not change. The present photocross-linking studies where the visual transduction pathway has been traced in a temperature-resolved rather than a time-resolved manner should be applicable to other GPCRs.

References and Notes

1. R. R. Rando, *Chem. Biol.* **3**, 255 (1996).
2. T. P. Sakmar, *Prog. Nucleic Acid Res. Mol. Biol.* **39**, 1 (1998).
3. D. Kliger and J. Lewis, *Isr. J. Chem.* **35**, 289 (1995).
4. T. Yoshizawa and S. Horiuchi, Eds., *Biochemistry and Physiology of Visual Pigments* (Springer-Verlag, New York, 1973).
5. A. Albeck *et al.*, *Biophys. J.* **55**, 233 (1989).
6. S. J. Hug, J. W. Lewis, C. M. Einterz, T. E. Thorgeirsson, D. S. Kliger, *Biochemistry* **29**, 1475 (1990).
7. H. Z. Zhang *et al.*, *J. Am. Chem. Soc.* **116**, 10165 (1994).
8. T. A. Nakayama and H. G. Khorana, *J. Biol. Chem.* **265**, 15762 (1990).
9. D. L. Farrens, C. Altenbach, K. Yang, W. L. Hubbell, H. G. Khorana, *Science* **274**, 768 (1996).
10. M. Han, S. W. Lin, M. Minkova, S. O. Smith, T. P. Sakmar, *J. Biol. Chem.* **271**, 32337 (1996).
11. M. Han, J. Lou, K. Nakanishi, T. P. Sakmar, S. O. Smith, *J. Biol. Chem.* **272**, 23081 (1997).
12. S. P. Sheikh, T. A. Zvyaga, O. Lichtarge, T. P. Sakmar, H. R. Bourne, *Nature* **383**, 347 (1996).
13. B. Borhan, M. L. Souto, J. M. Um, B. Zhou, K. Nakanishi, *Chem. Eur. J.* **5**, 1172 (1999).
14. M. L. Souto, J. Um, B. Borhan, K. Nakanishi, in preparation.
15. M. Ito, Y. Katsuta, Y. Imamoto, Y. Shichida, T. Yoshizawa, *Photochem. Photobiol.* **56**, 915 (1992).
16. Q. Tan, J. Lou, B. Borhan, E. Karnaukhova, N. Berova, K. Nakanishi, *Angew. Chem. Int. Ed. Engl.* **36**, 2089 (1997).
17. L. Oliveira, A. C. M. Paiva, C. Sander, G. Vriend, *Trends Pharmacol. Sci.* **15**, 170 (1994).
18. C. F. X. Schertler and P. A. Hargrave, *Proc. Natl. Acad. Sci. U.S.A.* **92**, 11578 (1995).
19. J. M. Baldwin, G. F. X. Schertler, V. M. Unger, *J. Mol. Biol.* **272**, 144 (1997).
20. I. D. Pogozheva, A. L. Lomize, H. I. Mosberg, *Biophys. J.* **72**, 1963 (1997).
21. T. Shieh, M. Han, T. P. Sakmar, S. O. Smith, *J. Mol. Biol.* **269**, 373 (1997).
22. P. Herzyk and R. E. Hubbard, *J. Mol. Biol.* **281**, 741 (1998).
23. Y. Shichida *et al.*, *Biochemistry* **26**, 4422 (1987).
24. R. H. Callender, A. Doukas, R. Crouch, K. Nakanishi, *Biochemistry* **15**, 1621 (1976).
25. G. Eyring, B. Curry, A. Broek, J. Lugtenburg, R. Mathies, *Biochemistry* **21**, 384 (1982).
26. S. O. Smith, J. Courtin, H. de Groot, R. Gebhard, J. Lugtenburg, *Biochemistry* **30**, 7409 (1991).
27. K. A. Bagley *et al.*, *Biochemistry* **24**, 6055 (1985).
28. H. Deng *et al.*, *Biochemistry* **30**, 4495 (1991).
29. I. Palings, E. M. M. van den Berg, J. Lugtenburg, R. A. Mathies, *Biochemistry* **28**, 1498 (1989).
30. A. Cooper, *Nature* **282**, 531 (1979).
31. G. A. Schick, T. M. Cooper, R. A. Holloway, L. P. Murray, R. R. Birge, *Biochemistry* **26**, 2556 (1987).
32. T. Yoshizawa and Y. Shichida, *Methods Enzymol.* **81**, 333 (1982).
33. M. Han, M. Groesbeek, T. P. Sakmar, S. O. Smith, *Proc. Natl. Acad. Sci. U.S.A.* **94**, 13442 (1997).
34. T. Okada, T. Matsuda, H. Kandori, Y. Fukada, T. Yoshizawa, Y. Shichida, *Biochemistry* **33**, 4940 (1994).
35. A. B. Asenjo, J. Rim, D. D. Oprian, *Neuron* **12**, 1131 (1994).
36. S. W. Lin and T. P. Sakmar, *Biochemistry* **35**, 11149 (1996).
37. L. A. Peteanau, R. W. Schoenlein, Q. Wasng, R. A. Mathies, C. V. Shank, *Proc. Natl. Acad. Sci. U.S.A.* **90**, 11762 (1993).
38. H. Chosrowjan *et al.*, *J. Am. Chem. Soc.* **120**, 9706 (1998).

39. Supported by NIH GM34509 (to K.N.) and Monbusho, Japan (to Y.S.). Thanks to M. Sheves and T. P. Sakmar for discussions.

30 December 1999; accepted 28 April 2000

Bacterial Mode of Replication with Eukaryotic-Like Machinery in a Hyperthermophilic Archaeon

Hannu Myllykallio,[1] Philippe Lopez,[2] Purificación López-García,[1]* Roland Heilig,[3] William Saurin,[3] Yvan Zivanovic,[1] Hervé Philippe,[2] Patrick Forterre[1]†

Despite a rapid increase in the amount of available archaeal sequence information, little is known about the duplication of genetic material in the third domain of life. We identified a single origin of bidirectional replication in *Pyrococcus abyssi* by means of in silico analyses of cumulative oligomer skew and the identification of an early replicating chromosomal segment. The replication origin in three *Pyrococcus* species was found to be highly conserved, and several eukaryotic-like DNA replication genes were clustered around it. As in Bacteria, the chromosomal region containing the replication terminus was a hot spot of genome shuffling. Thus, although bacterial and archaeal replication proteins differ profoundly, they are used to replicate chromosomes in a similar manner in both prokaryotic domains.

Recently, comparative genomics has revealed that most archaeal informational processes are similar to those in eukaryotes (*1*). This is especially striking in the case of DNA replication because all putative archaeal DNA replication proteins have eukaryotic homologs only or, alternatively, are more closely related to their eukaryotic counterparts

than to their bacterial ones (*2, 3*). The lack of conservation of replication factors in Eukarya/Archaea and Bacteria is so striking that their independent development after divergence from a last universal ancestor carrying an RNA genome has been suggested (*3*). Although recent experimental studies have confirmed predicted enzymatic activities for many open reading frames suggested to encode archaeal replication proteins (*4*), the processes through which chromosomes are replicated by these proteins have remained enigmatic. Even whether Archaea have a single replication origin, like Bacteria, or multiple origins, like Eukarya, has been unknown. In some bacteria, GC skew can be used to detect replication origins and termini due to an excess of G over C in the leading strand of replication (*5*). Conventional GC skew analyses failed to identify strand asymmetry in completely sequenced archaeal genomes (*6*), suggesting the possibility of multiple origins, in agreement with the eukaryotic nature of the archaeal replication apparatus. However, a single replication origin was suggested by cumulative diagrams of GC or tetramer skews in the Archaea *Methanobacterium thermoautotrophicum* (*7, 8*) and *Pyrococcus horikoshii* (*8*).

The genome of *P. abyssi* has been recently sequenced (*9*), allowing the comparison of strand asymmetry in the genomes of two closely related organisms (*P. abyssi* and *P. horikoshii*) in which major chromosomal rearrangements have occurred after their divergence (Fig. 1A). Although normal diagrams of oligomer skew (here, tetramer GGGT) could suggest multiple origins (Fig. 1B), cumulative skew analyses of the same tetramer gave smooth curves for the two genomes with one well-defined singularity and one broad peak, both at similar locations. The cumulative skew pattern thus appears to be a stable feature of genome composition because it has not been altered by the chromosomal rearrangements between the two *Pyrococcus* species (Fig. 1A). Similar results (*10*) were obtained when the genome sequence of a third *Pyrococcus* species, *P. furiosus*, was analyzed (*11*).

The shape of the cumulative skew diagrams in Fig. 1B could be explained a priori by two different replication mechanisms: one of the two singularities could represent a bidirectional replication origin, or they both could represent monodirectional replication origins. To distinguish between these possibilities, we sought to identify an early replicating chromosome segment with information deduced from the complete genome sequence of *P. abyssi*. In preliminary experiments, we found that uracil, but not thymidine, could be used to efficiently label chromosomal DNA when cells were grown anaerobically at 95°C (*12*). DNA synthesis in vivo was fully inhibited by puromycin, a universal protein synthesis inhibitor (Fig. 2). By analogy to the bacterial system, the residual incorporation of label into DNA observed in the presence of puromycin suggested that this inhibitor specifically blocks the initiation step of DNA replication in *P. abyssi*.

In a further experiment, DNA replication was arrested by puromycin, in order to increase the proportion of replication forks located close to the origin. After drug removal, newly replicating DNA was radioactively labeled, and the chromosomal distribution of radioactivity was determined by calculating the relative abundance of labeled Not I fragments of *P. abyssi*, as resolved by contour-clamped homogenous electric field electrophoreses (CHEFs) (*12*). After 30 min of labeling, the highest relative intensity was reproducibly observed for the 80-kb fragment (fragment II in Fig. 3), corresponding to the well-defined singularity present in skew diagrams (marked with the arrow in Figs. 1 and

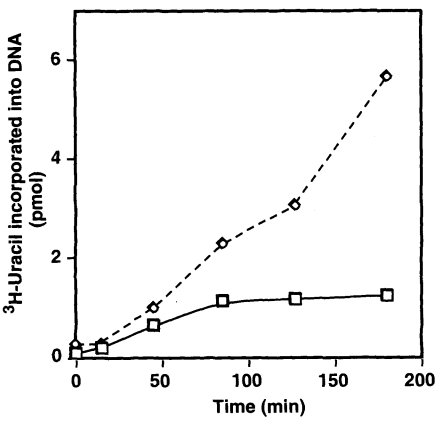

Fig. 2. Incorporation of ^{3}H-labeled uracil into an alkaline-resistant form (DNA) of *P. abyssi* in the absence (control, dashed line with diamonds) and presence of puromycin (200 μg/ml) (line with squares) is shown. Control experiments (*10*) using alkaline lysis and deoxyribonuclease I treatments of isolated nucleic acids from labeled cultures indicated that 30 to 35% of the label was incorporated into DNA. Incorporation of radioactive uracil was measured after trichloroacetic acid precipitation of whole cells by scintillation counting.

[1]Institut de Génétique et Microbiologie, [2]Laboratoire de Biologie Cellulaire, Université de Paris-Sud, 91405 Orsay Cedex, France. [3]Génoscope, Centre National de Séquençage, Evry, France.

*Present address: Department of Microbiology, Universidad Miguel Hernández, 03550 San Juan de Alicante, Spain.

†To whom correspondence should be addressed. E-mail: forterre@igmors.u-psud.fr

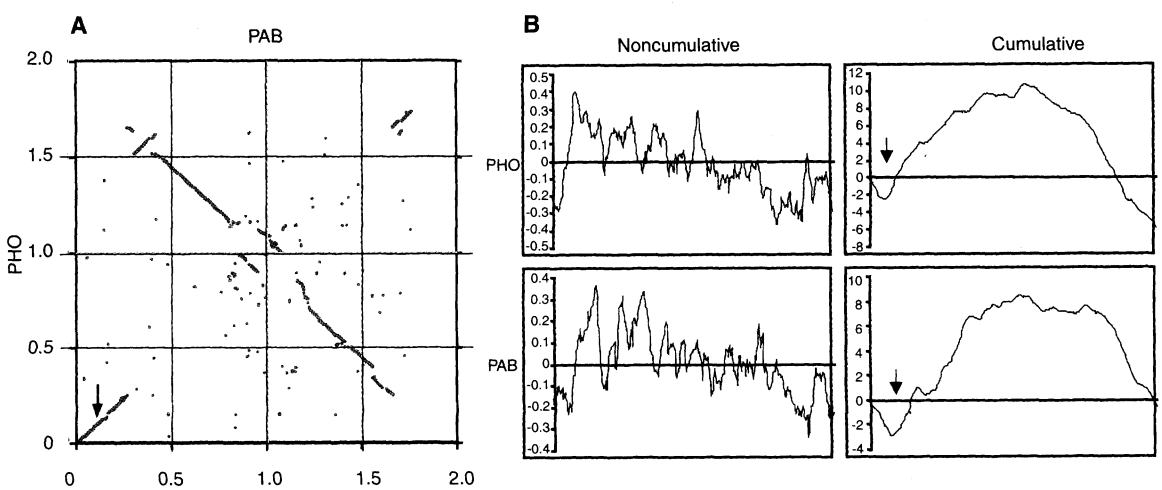

Fig. 1. (**A**) *Pyrococcus* genomes (PHO, *P. horikoshii*; PAB, *P. abyssi*) were compared using a BLAST tool and plotted against each other. Each data point represents 100 nucleotides with >80% identity between two genomes. Scale is given in increments of 10^6 bp. (**B**) Noncumulative (left) and cumulative (right) skews of tetramer GGGT for the two *Pyrococcus* genomes. In each graph, the abscissa represents the whole length of the genome and is directly comparable to those in (A). The skews are defined as the relative excess of tetramer GGGT over its reverse complement ACCC in a sliding window of 1/50th of the genome. The position of the window is incremented by 1/240th of the genome, yielding 240 values. Obtained values are displayed as shown for the noncumulative skew. The values were also integrated from the start of the genome, with positive and negative values resulting in an ascending and a descending slope, respectively. As expected, cumulative diagrams provide a much more convenient and accurate display of the trends of the skew. In the genome of *P. horikoshii* and *P. abyssi*, a well-defined singularity point is detected (indicated by the arrows).

3). The lowest value was obtained for the fragment located opposite fragment II on the *P. abyssi* genome, corresponding to the broad peak of the cumulative skew diagram. As expected for an early replicating fragment, the relative labeling intensity of fragment II gradually decreased when labeling was continued for up to 90 min. The simplest explanation for our in silico and experimental data is thus that *Pyrococcus* sp. chromosomes are replicated bidirectionally from a fixed single origin located within the 80-kb fragment described above and that the replication terminus is located approximately opposite the origin. Finally, the experimentally mapped replication origin of *P. abyssi* corresponds to a transition from negative to positive GC skew, indicating an excess of G over C in the leading strand of these Archaea (*5*).

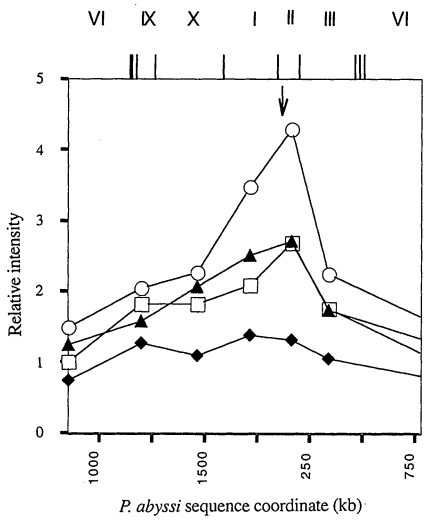

Fig. 3. Relative labeling intensities for *P. abyssi* Not I macrorestriction fragments are given. The abscissa indicates the middle point of the different fragments (indicated by roman numerals at the top) in sequence coordinates. The relative intensity of each fragment is plotted for three different time points of radioactive labeling (30 min, line with circles; 60 min, line with triangles; 90 min, line with diamonds) and for fluorescent detection without puromycin treatment (line with squares). All curves have a minimal value of 1.0 but have been offset by increments of 0.25 for readability. The location of the well-defined singularity of Fig. 1 is marked by the arrow.

The archaeal replication origin region that we identified does not contain typical sequences recognized by the bacterial initiator protein, nor is DnaA obvious in archaeal genomes (*2*). Instead, they all contain an archaeal homolog of Orc1/Cdc6 proteins that are involved in the initiation step of DNA replication in eukaryotes [reviewed in (*13*)]. These archaeal Orc1/Cdc6 homologs are located immediately downstream of a large intergenic sequence [~800 base pairs (bp)] (*14*). This is the only highly conserved intergenic sequence of >600 bp to be conserved in the three *Pyrococcus* genomes (*15*), suggesting a strong functional constraint for this region. This sequence contains a 45-bp central core with a single-nucleotide substitution between all three species, as well as many conserved direct and inverted repeats, similar to those present in the predicted origin of *M. thermoautotrophicum* [(*8*); see also Web fig. 1 (*16*)]. In the three *Pyrococcus* species, the described origin region carries many genes encoding orthologs of proteins involved in both the initiation (e.g., Cdc6/Orc1) and the elongation steps of eukaryotic DNA replication [e.g., replication factor C (RF-C)] (Fig. 4). Grouping of replication genes near the origin has been reported in some bacteria and possibly helps the effective assembly of replication forks onto the origin (*17*).

Whereas the replication origin is highly conserved between the three *Pyrococcus* species, the chromosomal region containing the replication terminus is a hot spot of genome shuffling, as shown by the genome-to-genome comparison between *P. abyssi* and *P. horikoshii* (Fig. 1A). Genetic instability in the terminus region has been also observed for Bacteria (*18*), and it could reflect a common mechanism for the termination of replication and/or chromosome segregation in all prokaryotes. Indeed, in addition to bacterial-like cell division genes already detected in Archaea [e.g., *ftsZ, minD*, and *spoJ* (*8*)], we noticed that *Pyrococcus* sp. and other Archaea contain a XerC and XerD homolog (PAB0255 in *P. abyssi*), which in Bacteria are involved in the resolution of chromosomes at the end of the replication process (*19*).

The successful identification of an archaeal replication origin validates the use of archaeal replication proteins such as Cdc6/Orc1 and minichromosome maintenance complex (MCM) to understand the functioning of their eukaryotic homologs (*20*). Because the genome of *P. abyssi* encodes only two putative initiator proteins (MCM and Cdc6/Orc1) in comparison to the complex set of proteins involved in yeast replication initiation, the archaeal in vitro replication system could represent a minimal eukaryotic-like mechanism for initiation of DNA replication. By itself, the replication of a prokaryotic chromosome from a single bidirectional replication origin by eukaryotic-like machinery raises fundamental questions. For example, our data indicate that the *P. abyssi* chromosome is replicated in ~45 min, i.e., once during every cell division. In this species, each replication fork must then be traveling at ~20 kb/min along the archaeal chromosome. This value is much higher than those observed for Eukarya (2 to 3 kb/min), although similar values have been obtained for Bacteria [*Escherichia coli*, 50 kb/min; *Caulobacter crescentus*, 21 kb/min (*21*)]. The faster replication rate in Archaea, as compared to that in Eukarya, could reflect the differences between the two replication apparatus [e.g., different replicative DNA polymerase and streamlining of several factors (*2*)] or a less compact nucleosomal structure (as expected for an actively transcribed genome with a high coding capacity).

We failed to identify strand asymmetry by cumulative skew or tetramer analyses in the genomes of *Methanococcus jannashii*, *Archaeoglobus fulgidus*, and *Aeropyrum pernix* and in some bacteria (*22*). Whether this implies the presence of multiple replication origins in these organisms or a limitation of the cumulative skew method remains to be established. However, the identification of both eukaryal and bacterial features in the *Pyrococcus* DNA replication mechanism already has evolutionary implications. The differences between replication factors in Eukarya/Archaea and Bacteria have been explained by (i) their high evolutionary rate triggered by the different replication modes in Eukarya and Bacteria (*1*), (ii) an independent development after their divergence (*3*), or (iii) a massive nonorthologous displace-

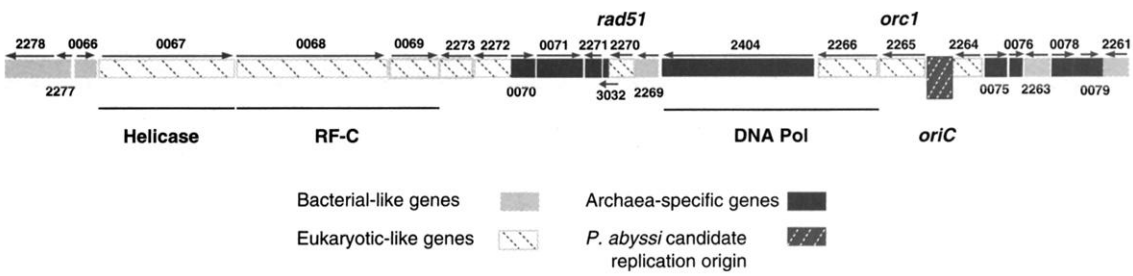

Fig. 4. A physical map of the *P. abyssi* origin region. The presence of genes for an archaeal initiator (Orc1/Cdc6), two subunits of DNA polymerase (DNA Pol), DNA polymerase processivity factor (RF-C), a Rad51 homolog, and putative DNA helicase in the vicinity of the *P. abyssi oriC* are indicated. Numbers indicate annotated open reading frames in the *P. abyssi* genome (*9*).

ment (*23*). Because, in the case of *P. abyssi*, eukaryotic-like replication proteins are used in a manner similar to that in Bacteria, the first possibility is unlikely. It remains to be established if similarities of archaeal and bacterial replication systems are a consequence of their common prokaryotic life-style (convergence) or if they are evolutionarily related (homologous). The latter hypothesis is supported by the observation that DnaA and Orc1/Cdc6 belong to the same protein superfamily (*24*), suggesting that all cellular replication initiation mechanisms originated in a DNA-based ancestor.

References and Notes

1. G. J. Olsen and C. R. Woese, *Cell* **89**, 991 (1997); D. R. Edgell and W. F. Doolittle, *Cell* **89**, 995 (1997).
2. R. Bernander, *Mol. Microbiol.* **29**, 955 (1998); I. K. Cann and Y. Ishino, *Genetics* **152**, 1249 (1999).
3. D. D. Leipe, L. Aravind, E. V. Koonin, *Nucleic Acids Res.* **27**, 3389 (1999).
4. I. K. Cann *et al.*, *J. Bacteriol.* **181**, 6591 (1999); Z. Kelman, S. Petrokovski, J. Hurwitz, *J. Biol. Chem.* **274**, 28751 (1999); G. Desogus, S. Onesti, P. Brick, P. Rossi, F. M. Pisani, *Nucleic Acids Res.* **27**, 4444 (1999); T. J. Kelly, P. Simancek, G. S. Brush, *Proc. Natl. Acad. Sci. U.S.A.* **95**, 14634 (1998).
5. J. R. Lobry, *Mol. Biol. Evol.* **13**, 660 (1996).
6. J. Mrazek and S. Karlin, *Proc. Natl. Acad. Sci. U.S.A.* **95**, 3720 (1998); S. Karlin, *Trends Microbiol.* **7**, 305 (1999).
7. A. Grigoriev, *Nucleic Acids Res.* **26**, 2286 (1998). In the case of *M. thermoautotrophicum*, one replication origin has been also predicted with an independent method [E. P. C. Rocha, A. Danchin, A. Viari, *Mol. Microbiol.* **32**, 11 (1999)].
8. P. Lopez, H. Myllykallio, H. Philippe, P. Forterre, *Mol. Microbiol.* **32**, 883 (1999).
9. The genome sequence of *P. abyssi* is available at www.genoscope.cns.fr/cgi-bin/Pab.cgi.
10. H. Myllykallio *et al.*, data not shown.
11. D. L. Maeder *et al.*, *Genetics* **152**, 1299 (1999).
12. Briefly, *P. abyssi* cultures were grown using enriched Vent Sulfothermophiles medium to an optical density at 600 nm (OD_{600}) = 0.12 and were treated with puromycin (200 μg/ml) for 110 min. The drug was removed by extensive washes with growth medium at 4°C. Treated cells were then reinoculated to OD_{600} = 0.10 in the presence of ^{14}C-labeled uracil (2 μCi/ml), and labeling was continued for indicated times (Fig. 2). Agarose plugs for CHEF analyses (6.5 V/cm, a linear pulse ramp of 3 to 17 s for 20 hours, 14°C) were prepared from 5-ml cultures by using a modification of standard protocols. Gels and filters (1 to 2 weeks of exposure to Storage Phosphor screens) were analyzed with a Storm imaging system (Molecular Dynamics, Sunnyvale, CA). Radioactivity of each Not I fragment was determined by using ImageQuant software and following the manufacturer's recommendations. To ensure that the results obtained were not an artifact of the puromycin treatment, the relative steady-state levels of Not I fragments were also investigated in untreated early exponential stage cultures. In this case, CHEF gels were stained with VistraGreen (Molecular Dynamics), a DNA-specific fluorescence dye, and were directly scanned with a blue fluorescence mode of a Storm system. Relative frequencies for fragments were obtained by dividing the amount of radioactivity/fluorescence of a given band by its size calculated on the basis of the determined genome sequence. All analyzed signals were within a linear range of a Storm system. The given values were normalized to the minimal value of one arbitrary unit and are averages of two independent measurements.
13. J. Leatherwood, *Curr. Opin. Cell Biol.* **10**, 742 (1998).
14. This region is interrupted by several stop codons in the three *Pyrococcus* genomes, indicating that it does not contain genes that could have been missed during the genome annotation.
15. The genome of *P. abyssi* contains 38 intergenic regions that are longer than 600 bp. When run through the BLAST program, only seven of these yield an expect score of $<1.0 \times 10^{-10}$ against the *P. horikoshii* genome, whereas the origin region gets an expect score of 1.0×10^{-33}. The use of the TBLASTX program indicates that the high scores of the remaining six intergenic regions might be due to some hard-to-identify open reading frames.
16. Available at www.sciencemag.org/feature/data/1048232.shl.
17. N. Ogasawara *et al.*, in *The Bacterial Chromosome*, K. Drlica and M. Riley, Eds. (American Society for Microbiology, Washington, DC, 1990), pp. 287–299.
18. J. M. Louarn, J. Louarn, V. Francoise, J. Patte, *J. Bacteriol.* **173**, 5097 (1991); H. Bierne and B. Michel, *Mol. Microbiol.* **13**, 17 (1994).
19. G. Blakely *et al.*, *Cell* **75**, 351 (1993).
20. The MCM protein of *M. thermoautotrophicum* acts as an adenosine triphosphate–dependent 3′–5′ DNA helicase [Z. Kelman, J. K. Lee, J. Hurwitz, *Proc. Natl. Acad. Sci. U.S.A.* **96**, 14783 (1999); J. P. J Chong, M. K. Hayashi, M. N. Simon, R.-M. Xu, B. Stillman, *Proc. Natl. Acad. Sci. U.S.A.* **97**, 1530 (2000).
21. B. Stillman, in *DNA Replication in Eukaryotic Cells*, M. DePamphilis, Ed. (Cold Spring Harbor Laboratory Press, Cold Spring Harbor, NY, 1996), pp. 435–460; A. Dingwall and L. Shapiro, *Proc. Natl. Acad. Sci. U.S.A.* **86**, 119 (1989).
22. P. Lopez and H. Philippe, unpublished data.
23. P. Forterre, *Mol. Microbiol.* **33**, 457 (1999).
24. A. F. Neuwald, L. Aravind, J. L. Spounge, E. V. Koonin, *Genome Res.* **9**, 27 (1999).

25. This work was supported by research grants from the European Union (BIO-CT 96-0488) and the Association de Recherche contre le Cancer. H.M. acknowledges financial support from the European Union and thanks U. Liebl for helpful discussions. We thank J. Weissenbach and his staff for sequencing the complete genome of *P. abyssi*.

27 December 1999; accepted 19 April 2000

Requirement of Mis6 Centromere Connector for Localizing a CENP-A–Like Protein in Fission Yeast

Kohta Takahashi,[1,2,3] Ee Sin Chen,[1,2] Mitsuhiro Yanagida[1,2,3]*

Mammalian kinetochores contain the centromere-specific histone H3 variant CENP-A, whose incorporation into limited chromosomal regions may be important for centromere function and chromosome segregation during mitosis. However, regulation of CENP-A localization and its role have not been clear. Here we report that the fission yeast homolog SpCENP-A is essential for establishing centromere chromatin associated with equal chromosome segregation. SpCENP-A binding to the nonrepetitious inner centromeres depended on Mis6, an essential centromere connector protein acting during G_1-S phase of the cell cycle. Mis6 is likely required for recruiting SpCENP-A to form proper connection of sister centromeres.

The kinetochore is a chromosomal architecture serving as the attachment site for spindle microtubules and is crucial for directing faithful chromosome segregation during mitosis (*1*). Because mutations in Mis6 and Mis12, two essential centromere proteins of the fission yeast *Schizosaccharomyces pombe*, disrupt centromere chromatin and cause high frequencies of missegregation (*2*, *3*), it is thought that the composition and/or modifications of the nucleosomes underlying centromere chromatin might be altered. Both mammalian CENP-A and its budding yeast homolog Cse4 function as essential histone-like components of the centromere nucleosomes (*4*, *5*).

To assess the possible role of CENP-A in centromere integrity and function, the gene encoding the CENP-A homolog in *S. pombe* was identified (*6*). Sequencing revealed a putative histone H3 variant clone [designated SpCENP-A; the formal gene name is *cnp1*$^+$ (centromere protein 1)] (Fig. 1A) encoding a polypeptide of 120 amino acids (*6*) with 57, 53, and 48% identity to the fission yeast histone H3, the budding yeast Cse4, and human CENP-A, respectively.

To examine intracellular localization of SpCENP-A, we constructed a fusion gene comprised of SpCENP-A with its native promoter and green fluorescent protein (GFP) that we confirmed to be functional (*7*) and integrated into the genome. SpCENP-A–GFP was seen as single dots near the nuclear periphery in interphase cells (Fig. 1B, top row). Two or three dots were observed in prometaphase or metaphase cells (Fig. 1B, rows 2 and 3) and one dot was present per daughter nucleus in anaphase cells (Fig. 1B, rows 4 and 5). In mitotically arrested β-tubulin mutant *nda3-311* (*8*), a single centromere-like locus of GFP signal was seen on each of

[1]CREST Research Project, Japan Science and Technology Corporation. [2]Department of Biophysics, Graduate School of Science, [3]Department of Gene Mechanisms, Graduate School of Biostudies, Kyoto University, Kitashirakawa-Oiwakecho, Sakyo-ku, Kyoto 606-8502, Japan.

*To whom correspondence should be addressed. E-mail: yanagida@kozo.biophys.kyoto-u.ac.jp